JGR Oceans

RESEARCH ARTICLE
10.1029/2023JC019677

On the Origins of Open Ocean Oxygen Minimum Zones

Xabier Davila[1,2], Are Olsen[1,2], Siv K. Lauvset[2,3], Elaine L. McDonagh[2,3,4], Ailin Brakstad[1,2], and Geoffrey Gebbie[5]

[1]Geophysical Institute, University of Bergen, Bergen, Norway, [2]Bjerknes Centre for Climate Research, Bergen, Norway, [3]NORCE Norwegian Research Centre, Bergen, Norway, [4]National Oceanography Centre, Southampton, UK, [5]Department of Physical Oceanography, Woods Hole Oceanographic Institution, Woods Hole, MA, USA

Key Points:

- We determine the origins of Oxygen Minimum Zones (OMZs) in terms of sources of volume, oxygen, and oxygen-deficit
- High-latitude source regions have a key role in feeding OMZs with oxygen-deficit, at centennial to millennial timescales
- The oxygen-deficit in the OMZs originates mostly from remineralization outside the OMZs

Supporting Information:

Supporting Information may be found in the online version of this article.

Correspondence to:

X. Davila,
Xabier.Davila@uib.no

Citation:

Davila, X., Olsen, A., Lauvset, S. K., McDonagh, E. L., Brakstad, A., & Gebbie, G. (2023). On the origins of open ocean oxygen minimum zones. *Journal of Geophysical Research: Oceans*, *128*, e2023JC019677. https://doi.org/10.1029/2023JC019677

Received 20 JAN 2023
Accepted 4 AUG 2023

Author Contributions:

Conceptualization: Xabier Davila, Are Olsen, Siv K. Lauvset, Elaine L. McDonagh, Geoffrey Gebbie
Formal analysis: Xabier Davila
Investigation: Xabier Davila
Methodology: Xabier Davila, Are Olsen, Siv K. Lauvset, Elaine L. McDonagh, Ailin Brakstad, Geoffrey Gebbie
Supervision: Are Olsen, Siv K. Lauvset, Elaine L. McDonagh, Geoffrey Gebbie
Visualization: Xabier Davila
Writing – original draft: Xabier Davila, Are Olsen

Abstract Recent work suggests that Oxygen Minimum Zones (OMZs) are sustained by the supply of oxygen-poor waters rather than the export of organic matter from the local surface layer and its subsequent remineralization inside OMZs. However, the mechanisms that form and maintain OMZs are not well constrained, such as the origin of the oxygen that oxygenates OMZs, and the locations where oxygen consumption occurs. Here we use an observation-based transport matrix to determine the origins of open ocean OMZs in terms of (a) OMZ volume, (b) oxygen that survives remineralization and oxygenates OMZs, and (c) oxygen utilization in the interior ocean that contributes to the oxygen-deficit of OMZs. We also determine where the utilization of oxygen occurs along the pathways that ventilate the OMZs. Our results show that about half of the volume of OMZ waters originate in high-latitude regions, but most of their oxygen is utilized for remineralization before they reach OMZs. Instead, OMZs are mostly oxygenated by tropical, subtropical and intermediate waters formed in nearby regions. More than half of the utilization of oxygen occurs in the tropics and subtropics, while less than a third occurs within the OMZs themselves. We therefore suggest that, in steady-state, OMZs are primarily set by ocean circulation pathways that high-latitude deep and old water upwards, with relatively low oxygen content.

Plain Language Summary Oxygen Minimum Zones (OMZs) are regions in the ocean where the dissolved oxygen concentration is low enough that many animals cannot survive there. It is uncertain what processes dominate the formation of OMZs because oxygen measurements only tell us about their deficit in oxygen, not where the oxygen loss occurred. Recent studies suggest that the oxygen is consumed in waters away from the OMZs and then these oxygen-poor waters are transported inside. However, the exact locations where the oxygen consumption occurs are still uncertain. Here we use a model built on observations to show where the oxygen is coming from and where it is consumed. We find that most of the oxygen in the OMZs is coming from young waters originating in nearby regions, while old waters that are low in oxygen come from distant, high-latitude regions. The latter suggests that oxygen consumption originates outside the OMZs and is then transported inside, agreeing with previous studies. About half of this consumption occurs as waters resurface in the tropics and subtropics where they are exposed to organic matter. We also find that the location of the OMZs is determined mainly from where water masses that sink in the high latitudes eventually resurface.

1. Introduction

Oxygen Minimum Zones (OMZs) are dissolved oxygen (O_2) deficient layers in the ocean of great importance for marine ecosystems and biogeochemical cycles. At oxygen concentrations below 20 μmol kg^{-1}, denitrification takes place (Smethie, 1987), leading to the production of nitrous oxide, which is a powerful greenhouse gas that amplifies global warming (Keeling et al., 2010). Regions below 60 μmol kg^{-1} are effectively "dead zones" for many higher trophic level animals such as fish and crustaceans (Gray et al., 2002). OMZs are usually found at depths between 100 and 900 m with O_2 concentrations as low as 4.5 μmol kg^{-1} (Karstensen et al., 2008). Direct observations show that OMZs are expanding (Stramma et al., 2010; Zhou et al., 2022), yet the underlying mechanisms are unclear. While global warming is expected to decrease ocean ventilation in a more stratified ocean (Keeling & Garcia, 2002), the myriad feedbacks involved result in highly uncertain responses of OMZs (Frölicher et al., 2020; Fu, Primeau, et al., 2018). Changes in circulation and biology dictate the shift from contraction to expansion of OMZ in CMIP6 models. A more sluggish circulation results in the expansion of low oxygenated waters in the periphery, while a combination of circulation and biological changes explain the contraction of the core (Busecke et al., 2022). However, two key aspects that link changes in circulation and biology to changes at

Writing – review & editing: Xabier Davila, Are Olsen, Siv K. Lauvset, Elaine L. McDonagh, Ailin Brakstad, Geoffrey Gebbie

OMZs are generally unexplored, which are (a) the origin of the oxygen that survives remineralization and oxygenates OMZs, as well as (b) the interior locations where the oxygen is utilized. Determining the mixed layer and ocean interior sources of OMZs is the purpose of this contribution.

The location and intensity of OMZs, as well as their sensitivity to climate variability and change, are determined by the fine balance between mechanisms that regulate oxygen supply and demand (Fu, Primeau, et al., 2018). There are three mechanisms that can contribute to the oxygen-deficit of OMZs: (a) Typically, OMZs are located underneath high productivity upwelling areas (Helly & Levin, 2004), thus, export of a copious amount of organic material and its remineralization can generate the oxygen-deficit; (b) the location of OMZs often coincides with the so-called "shadow zones" of thermocline ventilation pathways (Luyten et al., 1983) such that a combination of average oxygen consumption and sluggish circulation can lead to low oxygen; and (c) ample oxygen consumption can occur along the pathways as water circulates from the surface ocean to OMZs, such that the water masses that enter OMZs may be already depleted in oxygen on arrival. Hydrographic studies now indicate that the third mechanism, the transport of low-oxygen waters into OMZs, is the dominant contribution to OMZs. Olson et al. (1993) suggested that the Arabian Sea OMZ is maintained by moderate consumption in waters with initially low oxygen concentrations. Similarly, Kalvelage et al. (2013) showed that coastal currents (e.g., Peru-Chilean Undercurrent, Czeschel et al., 2011) transport a low-oxygen signal generated by remineralization within the sediments, into the East Tropical South Pacific (ETSP) OMZ. Finally, Sonnerup et al. (2019) estimated carbon export rates and ventilation timescales in the ETSP OMZ based on transient tracers and suggested that this OMZ may be sustained by the input of low-oxygen water from the Peru-Chile coastal upwelling rather than local utilization.

More sophisticated methods, such as transport matrices that are generated by the inversion of either model output or observations, can be used to infer global ventilation pathways of OMZs. Fu, Bardin, and Primeau (2018) used a transport matrix based on the ocean circulation field of an Earth System Model to quantify how surface ocean regions ventilate the Pacific OMZs, as well as the associated timescales. Their findings highlight the importance of intermediate waters, in accordance with previous studies that show the importance of these waters in ventilating the subtropics (Jones et al., 2016; Shimizu et al., 2004; Sloyan et al., 2010). However, they did not diagnose the origin of their oxygen content. Recently, Holzer (2022) used the Ocean Circulation Inverse Model 2 (OCIM2; DeVries & Holzer, 2019) transport matrix to investigate the injection and fate of oxygen in the ocean, with specific attention given to the formation and sensitivities of the North Pacific (NP) Hypoxic Zone and the East Tropical North Pacific (ETNP) OMZ. They found that most of the oxygen-deficit in the NP Hypoxic Zone and ETNP originates in the upper ocean, at mid-latitudes and in the eastern Tropical Pacific. However, their analysis did not cover specifically the sources of all major OMZs. Here we use an observation-based transport matrix to take a closer look at the four major OMZs in the world ocean.

We use the Total Matrix Intercomparison (TMI) from Gebbie and Huybers (2012) to determine the sources of the four major OMZs: the ETSP, ETNP, NP and the Arabian Sea—Bay of Bengal (AS-BB) OMZ. We explore the mixed layer origin of volume, oxygen and oxygen-deficit for the different endmembers that ventilate OMZs as well as the mean transit or ventilation timescales. We also determine the interior locations where the OMZ oxygen-deficit originates. These locations constitute the remineralization pathways between the mixed layer and OMZs, as well as within OMZs. Our results provide an observation-based benchmark for the origin and sensitivity of OMZs that results from each of the pathways and their contribution to oxygen and oxygen-deficit.

2. Methods

2.1. The TMI Framework

In this section, we provide a brief review of the TMI framework as used in this study. The TMI is a water mass decomposition method developed by Gebbie and Huybers (2010, 2012) that diagnoses the circulation pathways that connect the inner ocean with the mixed layer. The TMI exploits the fact that the value of a water mass property in the interior ocean can be expressed as a linear combination of the properties in the neighboring grid cells:

$$c_i = \sum_{j=i}^{N} m_{ij} c_j + r q_i, \tag{1}$$

where $N = 6$ is the number of neighboring grid cells, m_{ij} is the fraction of water that originates from cell j with property c_j, and $\sum_{j=1}^{N} m_{ij} = 1$ for conservation of mass. The local source and sink for non-conservative properties

are expressed by q_i, a single interior remineralization source that relates oxygen and nutrients through a global fixed stoichiometric ratio of P:N:O = 1:15.5:−170 (Anderson & Sarmiento, 1994). Gebbie and Huybers (2010) expressed (Equation 1) in matrix form:

$$\mathbf{Ac} = \mathbf{d}, \tag{2}$$

where $\mathbf{c}$ is a vector of the three-dimensional tracer field and $\mathbf{A}$ is a matrix containing, a priori unknown, dimensionless mixing coefficients between grid cells, which result from the diffusive-advective water mass pathways. The vector $\mathbf{d}$ on the right-hand side of Equation 2 is the sum of mixed-layer boundary conditions $\mathbf{c_b}$ (optimized prescribed tracer concentrations in the mixed layer) and of the concentration $\mathbf{q}$ of tracer surplus or deficit generated within each grid cell by interior sources and sinks ($\mathbf{d} = \mathbf{c_b} + \mathbf{q}$). The field $\mathbf{q}$ is defined such that the surplus or deficit of the tracer concentration relative to its preformed concentration ($\mathbf{A}^{-1}\mathbf{c_b}$) is given by $-\mathbf{A}^{-1}\mathbf{q}$ (see below for the connection to oxygen-deficit).

The only known element in Equation 2 is the tracer distribution $\mathbf{c}$. Gebbie and Huybers (2010) used the climatological water property fields from Gouretski and Koltermann (2004) (potential temperature (θ), salinity, $\delta^{18}O_{sw}$, PO_4^{3-}, NO_3^- and O_2) to invert for $\mathbf{A}$, $\mathbf{q}$ and $\mathbf{c_b}$. Later on, the circulation rates were also constrained through radiocarbon ($\Delta^{14}C$) observations from Key et al. (2004). The resulting transport matrix encapsulates the modern-day ocean circulation rates, in steady-state, where no changes in circulation, solubility or biology are accounted for. There are altogether 74,064 grid cells distributed in 33 vertical levels with a horizontal resolution of 4° by 4°. In the mixed layer that represents $\mathbf{c_b}$, there are 16,550 grid cells distributed in $s = 2{,}806$ mixed layer boxes that represent a vertically homogeneous winter-time mixed layer for each horizontal grid cell. The depth of the mixed layer varies regionally, such that the number of vertical levels of grid cells in the mixed layer varies from 1 to 14.

Here, we use their ocean pathways $\mathbf{A}$, $\mathbf{q}$, and $\mathbf{c_b}$, as well as the transit time distribution within the pathways constrained by Gebbie and Huybers (2012). With these elements, the steady-state distribution of a tracer,—for example, oxygen (Section 2.3), can be obtained by inverting Equation 2 so that $\mathbf{c} = \mathbf{A}^{-1}\mathbf{d}$.

Similar to the ocean tracer distribution, the volume of the interior ocean originating from a given mixed layer box, $\mathbf{v_{tot}}$, can be estimated with Equation 2 by propagating a dye from s in succession. However, a computationally more efficient way is by volume integrating the rows of $\mathbf{A}^{-T}$, which is done by multiplying the inverse transpose of $\mathbf{A}$ by a vector containing the interior volume $\mathbf{v}$ (Gebbie & Huybers, 2011):

$$\mathbf{v_{tot}} = \mathbf{A}^{-T}\mathbf{v}_i \quad \text{where} \quad i \in \Omega. \tag{3}$$

When Ω is the entire interior ocean, the values of the vector $\mathbf{v_{tot}}$ that are located at surface correspond to the total volume originating from each mixed layer box in the entire interior ocean. This expression is derived as a sensitivity or "adjoint" problem (see auxiliary material in Gebbie & Huybers, 2011). In our case, Ω is each of the OMZs considered (see Section 2.3), so that we are only tracing the volume of the OMZs back to surface and masking the rest of the ocean. The values in $\mathbf{v_{tot}}$ corresponding to the interior ocean, match the amount of volume at Ω that crosses each interior grid cell i (Brakstad et al., 2023; Gebbie & Huybers, 2011).

The mean age or ventilation timescales $\bar{T}_{s,i}$ can be estimated by integrating the transit time distributions—i.e., the distribution of times t that it takes for mixed layer waters from s to arrive at an interior grid cell i, $G_{s,i}(t)$, constrained by Gebbie and Huybers (2012):

$$\bar{T}_{s,i} = \int_0^\infty tG_{s,i}(t)dt \quad \text{where} \quad i \in \Omega, \tag{4}$$

where G is the transit time distribution, similar to the boundary propagator or Green's function of Haine and Hall (2002) but normalized to time-integrate to unity $\int_0^\infty G(t)dt = 1$ (Gebbie & Huybers, 2012).

2.2. Calculations of OMZ Sources

To characterize the oceanic processes that lead to the formation of OMZs, we use the above equations and different combinations of prescribed boundary conditions and interior sources/sinks. Specifically, we calculate the origins of (a) OMZ volume, (b) oxygen that survives remineralization and oxygenates OMZs and (c) its counterpart, the amount of oxygen utilized, as well as (d) the mean transit timescales or ventilation timescales. These

results are presented in Section 3.1. We also determine the patterns of oxygen utilization that happen as the water travels from their mixed layer source regions to the various OMZs. We refer to these patterns as "remineralization pathways" and they are presented in Section 3.2.

We first present the dissolved oxygen distributions reconstructed by the TMI, for model evaluation purposes and to define the OMZs (Section 2.3). The oxygen distribution is given by inverting Equation 2 so that $O_2 = \mathbf{A}^{-1}\mathbf{d}$. In this context, the two elements that compose $\mathbf{d}$ are (a) the optimized boundary condition of oxygen $\mathbf{c_b}$, and (b) the deficit of oxygen generated in each interior grid cell, $\mathbf{q}$ (expressed in terms of μmol kg^{-1}), and represents the product of Oxygen Utilization Rates and the local residence times of waters in each grid cell (Note that true oxygen utilization (TOU), the difference between preformed and actual oxygen concentration (Ito et al., 2004), is given by $\mathrm{TOU} = -\mathbf{A}^{-1}\mathbf{q}$). Latitudinally averaged sections of $\mathbf{q}$ are presented in Figure S1 in Supporting Information S1.

The OMZs volume originating from each mixed layer box is given by the surface values of $\mathbf{v_{tot}}$ by Equation 3. Here, only the interior grid cells i within the OMZs ($i \in \Omega$) are traced back to their mixed layer origin.

The injection of oxygen across the base of the mixed layer that survives remineralization and reaches the OMZs, O_{2s}, is calculated with Equation 2, by integrating the contribution from each of the mixed layer box s to the interior ocean, individually. This is done by prescribing a boundary condition of oxygen at s and keeping remineralization $\mathbf{q}$ active in the entire interior ocean. We then invert for $\mathbf{c}$, from the resulting tracer field, O_{2s} is calculated by integrating the mass of oxygen over all i located within Ω:

$$O_{2s} = \sum_{i=0}^{N} O_{2s,i} \quad \text{where} \quad i \in \Omega. \tag{5}$$

The counterpart of the preformed oxygen that has survived remineralization and reaches Ω is the True Oxygen Utilization (TOU, Ito et al., 2004) of s-sourced oxygen, that is, the usual TOU partitioned by mixed layer origin. The injection of TOU of s-sourced is calculated in a similar way to Equation 5. We first calculate the amount of preformed oxygen injected from each mixed layer box into Ω, O^0_{2s}, by prescribing again a boundary condition of oxygen at s, but this time setting $q_i = 0$ everywhere, and integrating the resulting oxygen field over $i \in \Omega$. Then we calculate the TOU of s-sourced oxygen, $\Delta O_{2s} = O^0_{2s} - O_{2s}$.

The mean transit times are directly calculated from the transit time distribution, $G_{s,i}$, determined by Gebbie and Huybers (2012) with the difference that only the waters within the OMZ are traced ($i \in \Omega$). We also determine the mean age of the OMZs with Equation 4.

The remineralization pathways presented in Section 3.2 represent the along-path oxygen utilization ($\overrightarrow{\Delta O_{2s}}$; μmol kg^{-1}), and represents the total amount of oxygen utilized in each interior location i that was transported across the mixed layer in s and will contribute to the oxygen-deficit in Ω. $\overrightarrow{\Delta O_{2s}}$ is calculated by combining the oxygen sinks $\mathbf{q}$ and the density field ρ, with the global water pathways $\mathbf{v_{tot}}$ in Equation 3. This allows us to determine the oxygen utilized at each interior location on the paths that connect the mixed layer grid cell s with the OMZs. We call this the along-path oxygen utilization:

$$\overrightarrow{\Delta O_{2s}} = \mathbf{q} \cdot \mathbf{f_s} \cdot \rho \cdot \frac{\mathbf{v_{tot}}}{\mathbf{v}}, \tag{6}$$

where $\overrightarrow{\Delta O_{2s}}$ is a vector of a three-dimensional field and is the interior distribution of ΔO_{2s}, so that $\Delta O_{2s} = \sum_{i=0}^{N} \overrightarrow{\Delta O_{2s,i}}$, where i in this case is anywhere in the world ocean. The elements on the right-hand side are also vectors and are multiplied element-wise. The interior distribution of water mass fraction originating from s is represented by $\mathbf{f_s}$, and $\frac{\mathbf{v_{tot}}}{\mathbf{v}}$ normalizes the volume of the OMZs that cross each interior grid cell in $\mathbf{v_{tot}}$ with respect to the volume of each grid cell itself in $\mathbf{v}$, so that $\frac{\mathbf{v_{tot}}}{\mathbf{v}}$ indicates the fraction of $\mathbf{v}$ that ends up in the OMZ. In other words, Equation 6 quantifies the amount of water in each interior ocean grid cell that originates at s and is bound to arrive at an OMZ, combined with $\mathbf{q}$.

If s is the entire ocean mixed layer boxes, the totality of OMZ remineralization pathways are mapped (Section 3.2). If s is the mixed layer boxes at a defined endmember (e.g., North Atlantic), the remineralization pathways for that individual endmember can be quantified (Supporting Information S1). The water mass fraction is calculated with Equation 2 and prescribing a boundary condition of ones at the selected mixed layer boxes and zero elsewhere at surface, with no interior sources/sinks $q_i = 0$.

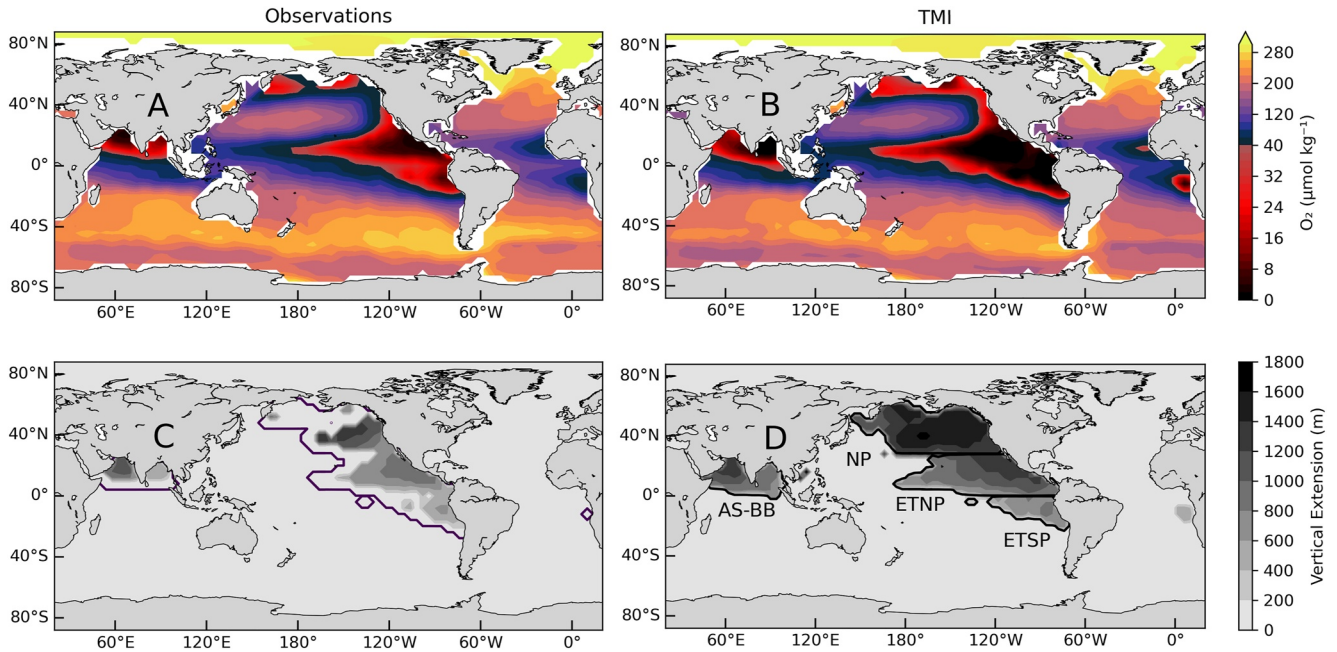

Figure 1. Oxygen concentration at 1,000 m depth from (a) observations and (b) the Total Matrix Intercomparison (TMI). The observed distribution is taken from the World Ocean Circulation Experiment (WOCE) data set (Gouretski & Koltermann, 2004), which was used to constrain the TMI. The modeled TMI distribution is calculated with Equation 2 and assuming a fixed stoichiometric ratio of P:O = 1:−170. The colorbar breaks at 40 μmol kg^{-1} to highlight the small gradients in the vicinity of the Oxygen Minimum Zones (OMZs). Horizontal and vertical extension of (c) observed and (d) modeled OMZs, defined as waters with oxygen levels <20 μmol kg^{-1}. The black contours in C indicate the maximum horizontal extension of OMZs when the observational error is taken into account. The four OMZs evaluated here are the Arabian Sea-Bay of Bengal (AS-BB), North Pacific (NP), East Tropical North Pacific (ETNP) and East Tropical South Pacific (ETSP).

2.3. Model Evaluation

The TMI reproduces the oxygen distribution appropriately with respect to the error of the observed climatology used to constrain it (Gebbie & Huybers, 2010; Gouretski & Koltermann, 2004). The modeled and observed climatological distributions are comparable, but the modeled concentrations are generally lower than observed (Figure 1). The TMI oxygen field is mostly biased toward the lower bound of the observational error. The mismatch is well within observational error in the upper ocean but worsens with depth, up to ∼10 times the observational error in the Southern Ocean (Figure S2 in Supporting Information S1).

The concentration gradients around OMZs are relatively small and the locations of OMZs are, as a consequence, very sensitive to the threshold used to define them. Additionally, biases of a few μmol kg^{-1} in the climatology can significantly affect the observed OMZ extension. Several factors contribute to potential error in the climatology, notably: (a) seasonal and interannual variability related to both circulation and biological export can affect the position and intensity of OMZs, and is typically highest in the first 1,000 m (Deutsch et al., 2011; Gouretski & Koltermann, 2004); (b) low oxygen levels such as in OMZs are close to the detection limit of available analytical methods (Bianchi et al., 2012); (c) the choice of spatial correlation when gap-filling discrete data points oversmooths data at small scales (Gouretski & Koltermann, 2004); and (d) evidence that gridded climatologies overestimate the oxygen concentrations and underestimate OMZs volume (Bianchi et al., 2012; Fuenzalida et al., 2009). On the other hand, the TMI is constrained using a climatological distribution and, as such, does not capture the co-variations between water mass formation and primary production. In addition, the oxygen distribution in the TMI is modeled assuming a fixed stoichiometric ratio of P:N:O = 1:15.5:−170, which we acknowledge is not representative for the entire ocean (Carter et al., 2021; Teng et al., 2014), in particular in the OMZs as the strong reduction-oxidation gradients lead to denitrification and to differences in the P:N:O ratios (DeVries et al., 2012). However, we note that the mismatches between the modeled and observed distributions are not particularly high for the OMZs when normalized by the observational error of the data used to constrain the TMI (Figure S2 in Supporting Information S1).

We use an oxygen concentration of 20 μmol kg^{-1} as a threshold for OMZs. We do note that there is no agreed threshold that defines an OMZ, however (Busecke et al., 2022; Karstensen et al., 2008; Paulmier & Ruiz-Pino, 2009),

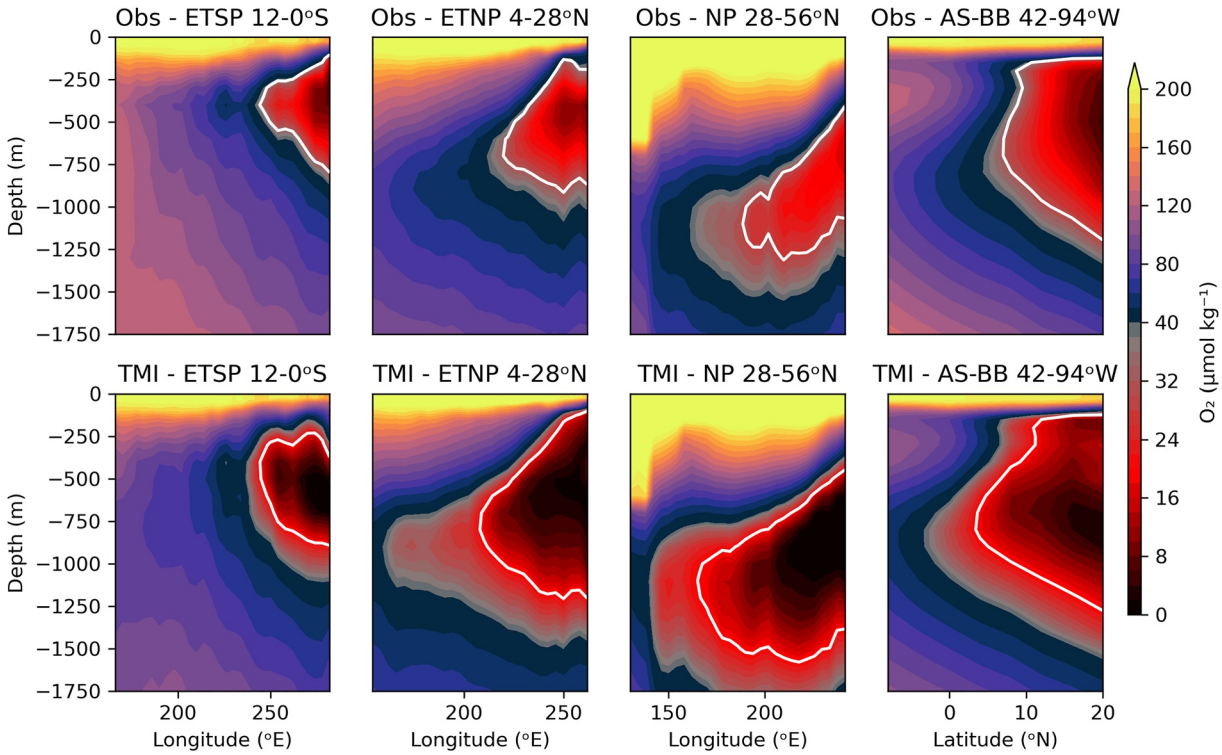

Figure 2. Meridionally averaged cross-sections of observed (top) and Total Matrix Intercomparison (TMI) (bottom) oxygen distributions in the water column for the East Tropical South Pacific, East Tropical North Pacific (NP) and NP Oxygen Minimum Zones (OMZs), and zonally averaged cross-section for the Arabian Sea—Bay of Bengal OMZ. The observed distribution is taken from the WOCE data set (Gouretski & Koltermann, 2004) used to constrain the TMI, The colorbar breaks at 40 µmol kg^{-1} to highlight the small concentration gradients in the vicinity of OMZs. The white contour that overlies the observations indicates the maximum extent of the observed OMZ when observational error is taken into account, and the location of the modeled OMZ for the modeled distributions.

and different studies use different thresholds depending on their goal. We decided to use 20 µmol kg^{-1} so our results are comparable to those of Fu, Bardin, and Primeau (2018) in terms of ventilation. This threshold also provides a good compromise between OMZ volume and the maximum concentration at which denitrification has been observed (Smethie, 1987), even if the definition of suboxic conditions is much lower (2–10 µmol kg^{-1}, Bianchi et al., 2012).

We focus on the four major OMZs: The ETSP, ETNP, NP and the Arabian Sea—Bay of Bengal (AS-BB). Because the TMI is biased toward slightly low oxygen concentrations, the modeled OMZs are larger both horizontally and vertically than the observed ones (Figures 1 and 2). Also, the modeled ETSP and ETNP OMZs are not as separated as in the observations, but two distinct cores are nevertheless visible. We set the border between the ETNP and NP to 38°N. This coincides with the steep deepening of the 20 µmol kg^{-1} isoline that separates these two OMZs (not shown). The position of the modeled AS-BB OMZ agrees well with the observations, but it extends slightly too far south. The TMI also models an East Tropical Atlantic OMZ, however, this is not visible in observations as concentrations are higher than 20 µmol kg^{-1} (Keeling et al., 2010). The East Tropical Atlantic OMZ is therefore left out from our analyses. For the NP OMZ, the observed size is significantly smaller than the modeled. Overall we conclude that the TMI, as constrained by available observations and their uncertainties, provides a qualitatively realistic representation of oxygen in the ocean despite some systematic quantitative differences.

3. Results

3.1. Mixed Layer Sources

The role of the various water mass formation regions for the oxygenation of OMZs is determined by the interplay of their volume contributions and oxygen concentrations. While every OMZ is slightly different, they share some general features. Most of the volume originates from high latitudes, from the formation of mode, intermediate and

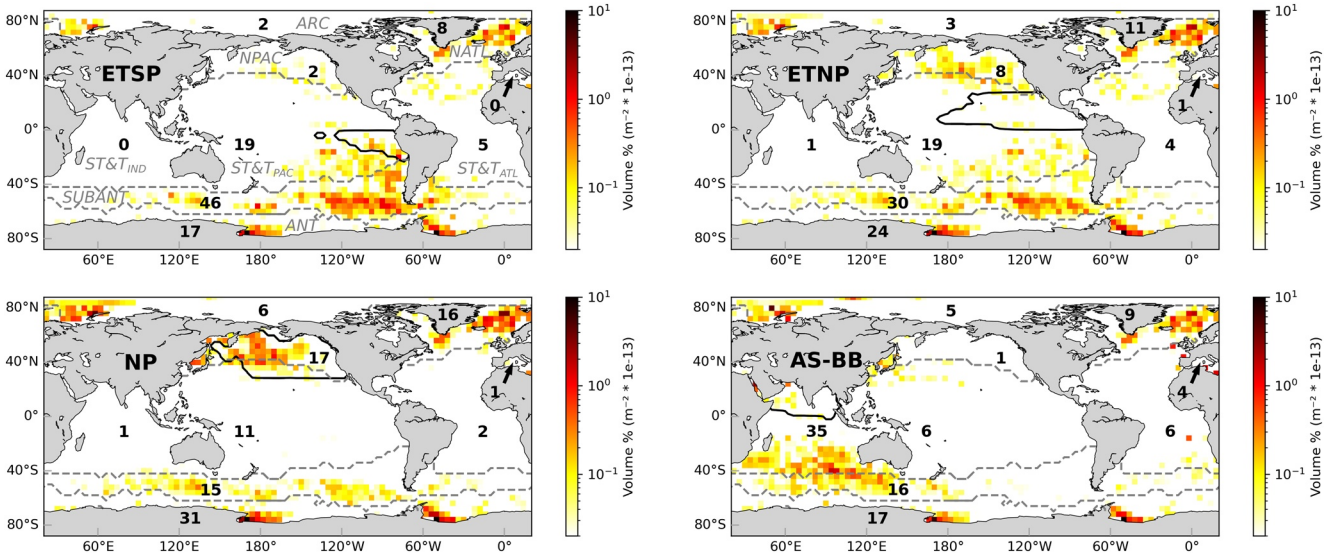

Figure 3. Fractional volume contributions of each mixed layer box to the Oxygen Minimum Zones (OMZs), based on the transit time distributions (Section 2.1; Gebbie & Huybers, 2012). Values below 0.02 $m^{-2} \times 10^{-13}$% are masked. Black contours show the location of the OMZs as defined in Figure 1. Gray dashed lines show the outcrop region for each of the source water masses defined as in Gebbie and Huybers (2012) and the black numbers represent the volume % when integrated over each outcrop region. The colorscale is logarithmic.

bottom waters (Figure 3). For the Pacific OMZs, waters from the Southern Ocean make up the bulk of the volume, formed either in the Subantarctic region as Mode/Intermediate Water (defined as the combination of Antarctic Intermediate Water and Subantarctic Mode Water) or in the Antarctic region as Antarctic Bottom Water. The relative importance of Subantarctic Mode/Intermediate Waters for the Pacific OMZs decreases from south (46% in ETSP) to north (15% in NP). Conversely, the relative contribution of Antarctic Bottom Water increases from 17% in the ETSP to 31% in the NP. This is in accordance with previous estimates of these water masses (DeVries & Primeau, 2011; Johnson, 2008). The fraction of water from the North Atlantic (North Atlantic Deep Water) also increases from south to north in the Pacific (from 8% in the ETSP to 16% in the NP). On the other hand, the NP region contributes more to the northern Pacific OMZs (17% in NP) and less to the southern OMZ (2% in ETSP). The combined contribution by the tropics and subtropics to the volume of OMZs is substantial, but always less than the combined contributions of high-latitude sourced waters. The AS-BB is the most unique of all OMZs in terms of source waters, as more than a third (35%) of the volume originates in the tropical and subtropical parts of the Indian Ocean. There are, nevertheless, substantial contributions from Antarctic Bottom Water (17%) and Subantarctic Mode/Intermediate Waters (16%) to the AS-BB. Overall, the waters present in OMZs stem mostly from the high latitudes, specifically through the formation of bottom and mode waters in the Southern Ocean. These waters contribute to about half of the volume of every OMZ except for the AS-BB where they contribute about one-third. The volumetric contributions from the mixed layer to the ETSP and ETNP, as well as its transit times, were also estimated by Fu, Bardin, and Primeau (2018) and the comparability of these estimates are discussed in Section 4.

The pattern of the oxygen injected across the base of the mixed layer that survives remineralization and reaches the OMZs (Figure 4) and its counterpart, the amount of injected oxygen that is utilized (Figure 5), follow the volume injection pattern largely. Endmembers adjacent to OMZs (i.e., Tropical and Subtropical regions) carry more oxygen than those further away from OMZs (i.e., the high latitudes) as waters from the latter have been subjected to more utilization and thus contribute more to OMZs' oxygen-deficit. For the Pacific OMZs, Subantarctic Mode/Intermediate Waters and NP Intermediate Waters are the main sources of oxygen that survives remineralization and is delivered to the OMZs. Similarly to water volume, the contribution to oxygenation by the Subantarctic Mode/Intermediate Waters endmember decreases from south to north, from 67% for ETSP to virtually zero for the NP. The contributions from the Antarctic region through the Antarctic Bottom Water, however, deviate from the volume pattern. The Antarctic Bottom Water barely contributes to oxygen supply for any OMZ, despite its large volume contribution, reflecting that a large part of the preformed oxygen has been utilized as this water mass travels from its formation regions to OMZs. This is apparent in the oxygen-deficit contributions (ΔO_2;

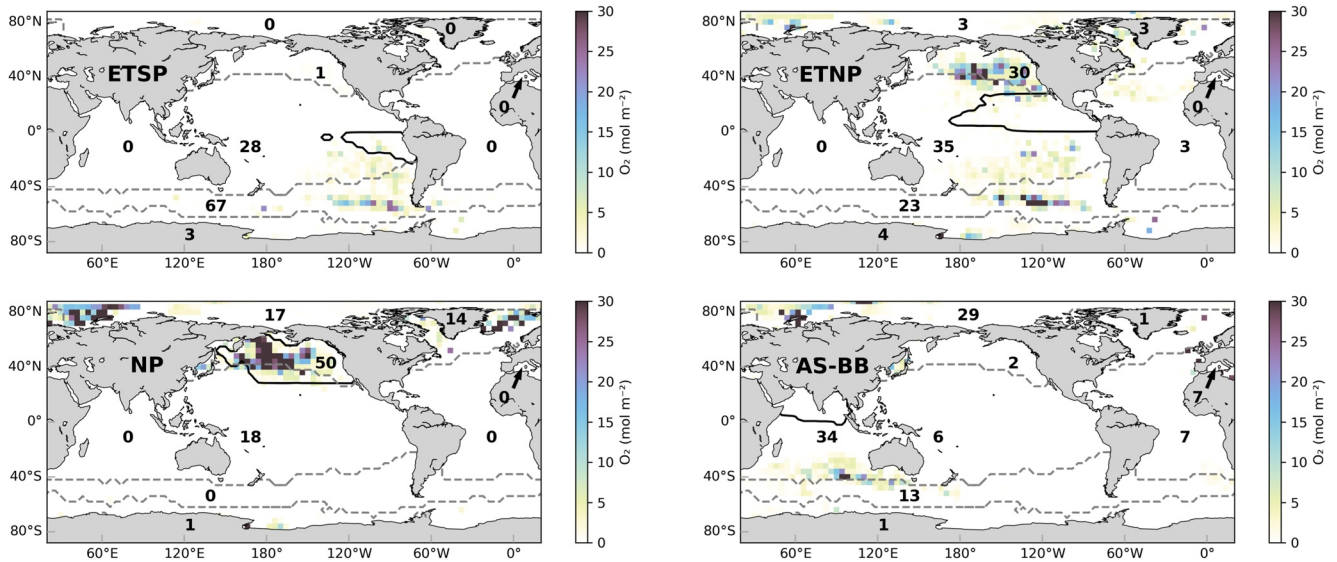

Figure 4. Injection of oxygen from each mixed layer box into the Oxygen Minimum Zones (OMZs). This oxygen survives remineralization and arrives in the OMZs. Black contours represent the location of the OMZs as defined in Figure 1. Gray dashed lines represent the outcrop regions for each of the source water masses defined as in Figure 3. The numbers are the contributions of each outcrop region to the total oxygen content in the OMZ, in %. The colorscale of the East Tropical South Pacific (ETSP) panel has a different range than the rest.

Figure 5). The North Atlantic is another region that barely contributes to oxygen as most of it has been utilized along-path; it contributes to the oxygen-deficit instead. In general, high-latitude waters are the most important contributors to oxygen-deficit and are in accordance with that of volume; the oxygen-deficit from the Antarctic Bottom Water increase from the southernmost OMZ in the Pacific (20% for ETSP) to the northernmost (35% for NP), and so does that of the North Atlantic endmember (from 10% for ETSP to 18% to NP). Intermediate waters from the Subantarctic and NP contribute to both oxygen-deficit and oxygenation. The oxygen-deficit contributions of Subantarctic Mode/Intermediate Waters to OMZs follow the same pattern as volume and oxygen, and decrease from the ETSP (45%) to NP (16%). Subtropical and Tropical waters, on the other hand, are more

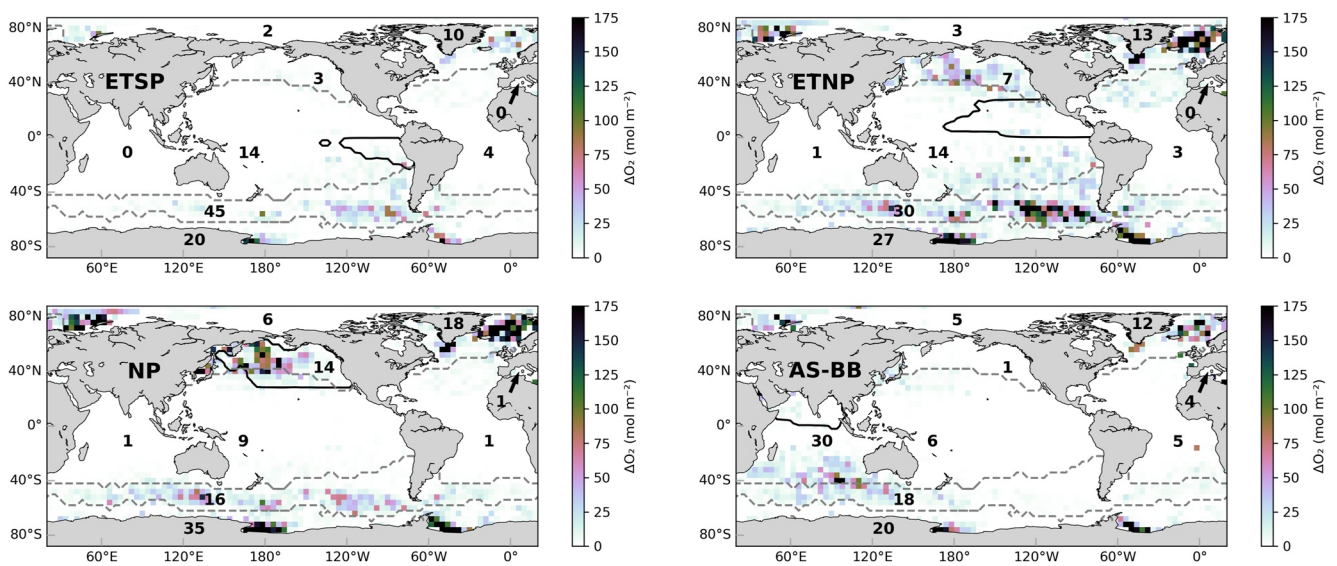

Figure 5. The injection of true oxygen utilization of *s*-sourced oxygen across the base of the mixed layer, or the oxygen that is bound to be utilized from each mixed layer box en route to each of the Oxygen Minimum Zones (OMZs). The integrated mass of oxygen utilized is equivalent to the total oxygen-deficit accumulated in each OMZ. Black and gray contours represent the same as in Figure 4. The numbers are the contributions of each outcrop region to the total oxygen-deficit in the OMZ, in %. The colorscale of the East Tropical South Pacific (ETSP) panel has a different range than the rest.

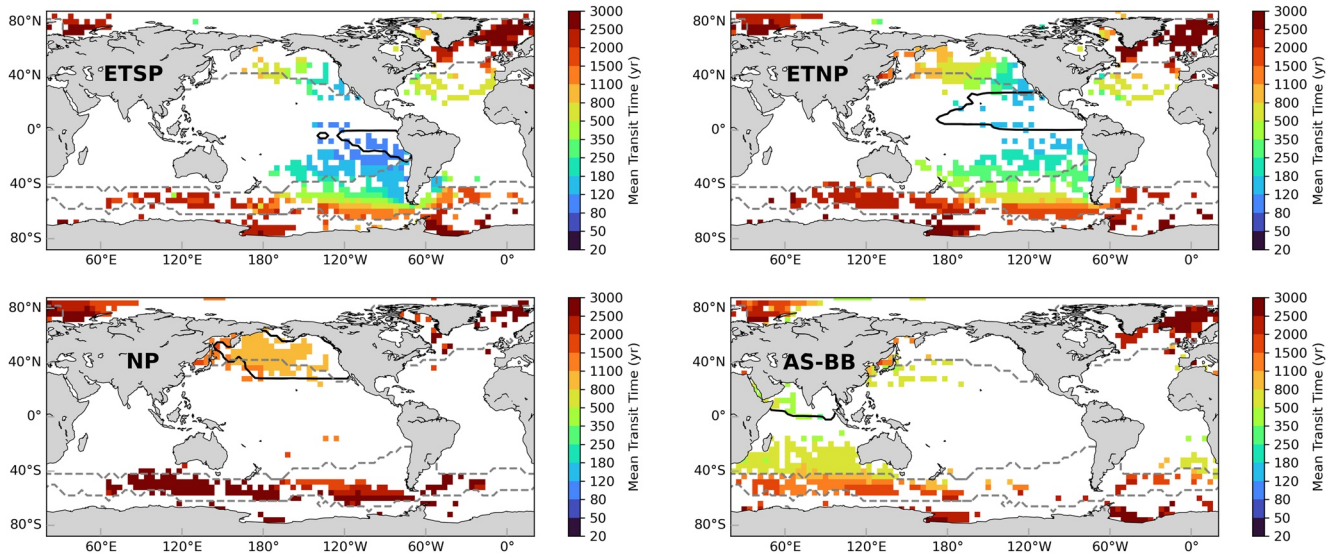

Figure 6. Mean transit time for the water from each mixed layer box to each of the Oxygen Minimum Zones (OMZs). Black and gray contours represent the same as in Figure 4. The same mask as in Figure 3 is applied, so that mixed layer boxes that do not contribute significantly to the OMZ volume are white.

important for oxygenation than for volume, reflecting the short pathways of these waters to OMZs. While these waters are the largest contributor to oxygen for the AS-BB (34%), they are also the largest contributor to the oxygen-deficit (30%, Figure 5). Surprisingly, the contribution of Arctic waters to the oxygenation of the AS-BB as well as the NP is also large, 30% and 18%, respectively. While surprising, this partly agrees with the findings presented in Holzer (2022) (discussed in Section 4) where part of the oxygen that is utilized within the NP Hypoxic Zone (PHZ) originates from the Arctic and North Atlantic. In general, the large amount of preformed oxygen injected by high-latitude endmembers as opposed to low-latitude ones, and its subsequent conversion to oxygen or oxygen-deficit, underscores the sensitivity of OMZs to high-latitude processes and the need for their correct representation, for example, in Earth System Models.

The regions that contribute most to the oxygen-deficit in OMZs are also those for which the transit times to the OMZs are the longest (Figure 6). The waters from these regions are subjected to remineralization for the longest time and thus have the highest total utilization of oxygen. The transit times of the water masses from their source regions to the OMZs range from decadal to millennial. Antarctic Bottom Water and North Atlantic Deep Water have the longest mean transit time from their source regions to the OMZs, about 3,000 years. The shortest mean transit times are from regions adjacent to the OMZs. Subtropical and Tropical waters arrive in the ETSP and ETNP OMZs at decadal timescales, while Subantarctic Mode/Intermediate Waters and NP Intermediate Water endmembers take centuries. Transit times are overall longer to the NP and AS-BB OMZs. The shortest ventilation timescale for the NP OMZ is about 1,000 years, by the NP Intermediate Water, and 500 years for the AS-BB OMZ, by Subtropical and Tropical waters. For both, the transit times of the other source waters (Subantarctic Mode/Intermediate Waters, Antarctic Bottom Water, North Atlantic Deep Water) are up to 3,000 years. The mean age of the OMZ is determined as the volume-weighted average of all the transit times. This is lowest for the AS-BB OMZ, ∼360 years, followed by the ETSP OMZ with ∼440 years, the ETNP OMZ with ∼610 years and the NP OMZ is the oldest with a mean age of ∼1,150 years.

3.2. Remineralization Pathways

Traditional metrics such as TOU measure the path-integrated oxygen-deficit at a specific location, meaning that the signature of ocean circulation and oxygen utilization are convolved. The TMI directly constrains the generated oxygen-deficit in each interior location, q_i, from the tracer distribution (Equation 1). This allows us to determine whether the oxygen utilization occurs near the water formation regions, in the OMZ itself, or on the path between the former and the latter. We call this the along-path oxygen utilization ($\overrightarrow{\Delta O_2}$ (μmol kg^{-1}); Section 2.2).

The vertically integrated distribution of $\overrightarrow{\Delta O_2}$ (Figure 7) is primarily dependent on the pathway that water masses follow from mixed layer to destination (Figure S3 in Supporting Information S1). In essence, $\mathbf{v}_{\mathbf{tot}}$ acts as a path

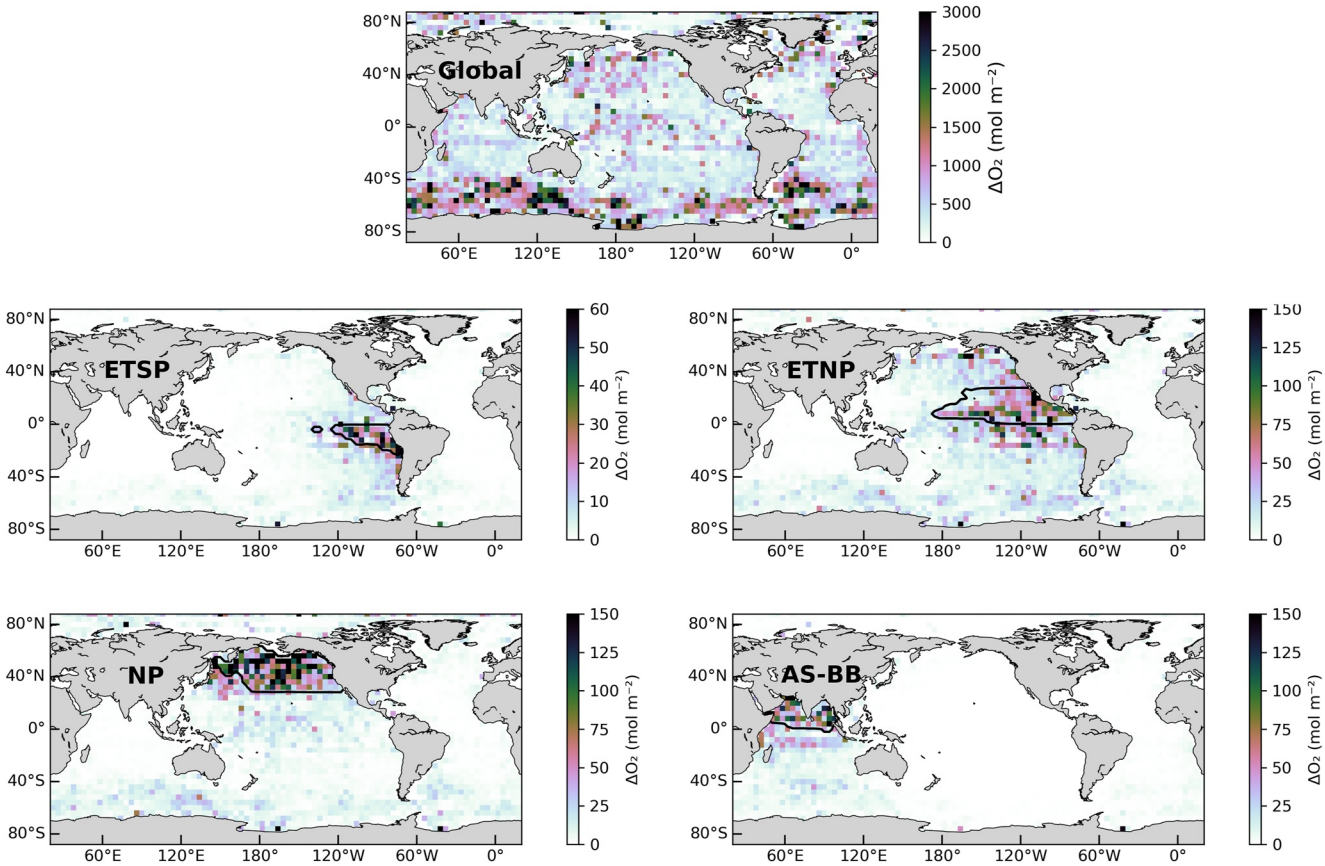

Figure 7. Vertically integrated $\overrightarrow{\Delta O_2}$ along the path that connects the global mixed layer with the global interior ocean and with each of the Oxygen Minimum Zones.

selector (Holzer, 2022) for the global $\overrightarrow{\Delta O_2}$ pattern (Figure 7), that is, the larger the volume of water en route to an OMZ in a given grid cell the larger the contribution of remineralization in that grid cell to the oxygen-deficit of the OMZ. $\overrightarrow{\Delta O_2}$ also expresses the sensitivity of the OMZs to remineralization, that is, how much would the oxygen-deficit in the OMZs change per unit of change in remineralization. As expected, per area of ocean, the OMZs are most sensitive to the remineralization that occurs around the OMZs (highest $\overrightarrow{\Delta O_2}$; Figure 7), however, this is because the volume fractions of waters bound to reach the OMZs are largest in the vicinity of the OMZs, and not because of local export production resulting in unusually large oxygen sinks. The OMZs do not stand out as regions with high $\overrightarrow{\Delta O_2}$ nor are they distinguishable from the rest of the ocean when the global ocean is taken as destination Ω (Figure 7—Global). The fact that OMZs are not regions of excessive oxygen utilization combined with the findings on the mixed layer sources (Section 3.1), suggests that the location of OMZs is governed by the geometry of the oceanic pathways, that is, OMZs are located in regions where old and dense deep waters gain enough buoyancy to return to the upper ocean (De Lavergne et al., 2017; Holzer et al., 2021; Primeau & Holzer, 2006).

We further investigate the regional distribution of oxygen consumption, from each source region to each of the four OMZs investigated here (Figure 8). Most of the $\overrightarrow{\Delta O_2}$ originates outside OMZs, with only less than a third occurring within. When the global ocean mixed layer is taken as a source, 17% of the oxygen-deficit within the ETSP is generated within the ETSP OMZ. This fraction is 17% for the ETNP, 22% for the NP, and 31% for the AS-BB. For the individual water mass pathways, the $\overrightarrow{\Delta O_2}$ generated within the OMZs is typically only around 10%–30%, with the exception of the AS-BB OMZ where these values are between 20% and 63%. The water masses originating at high latitudes and characterized by longer transit times tend to have a smaller fraction of the oxygen-deficit generated inside the OMZs compared to those with shorter transit times. However, these differences are generally small and, for almost every pathway, most of the oxygen is consumed in three regions (when including OMZs): (a) in the water mass formation regions themselves, (b) in the subtropics and tropics, and (c) in

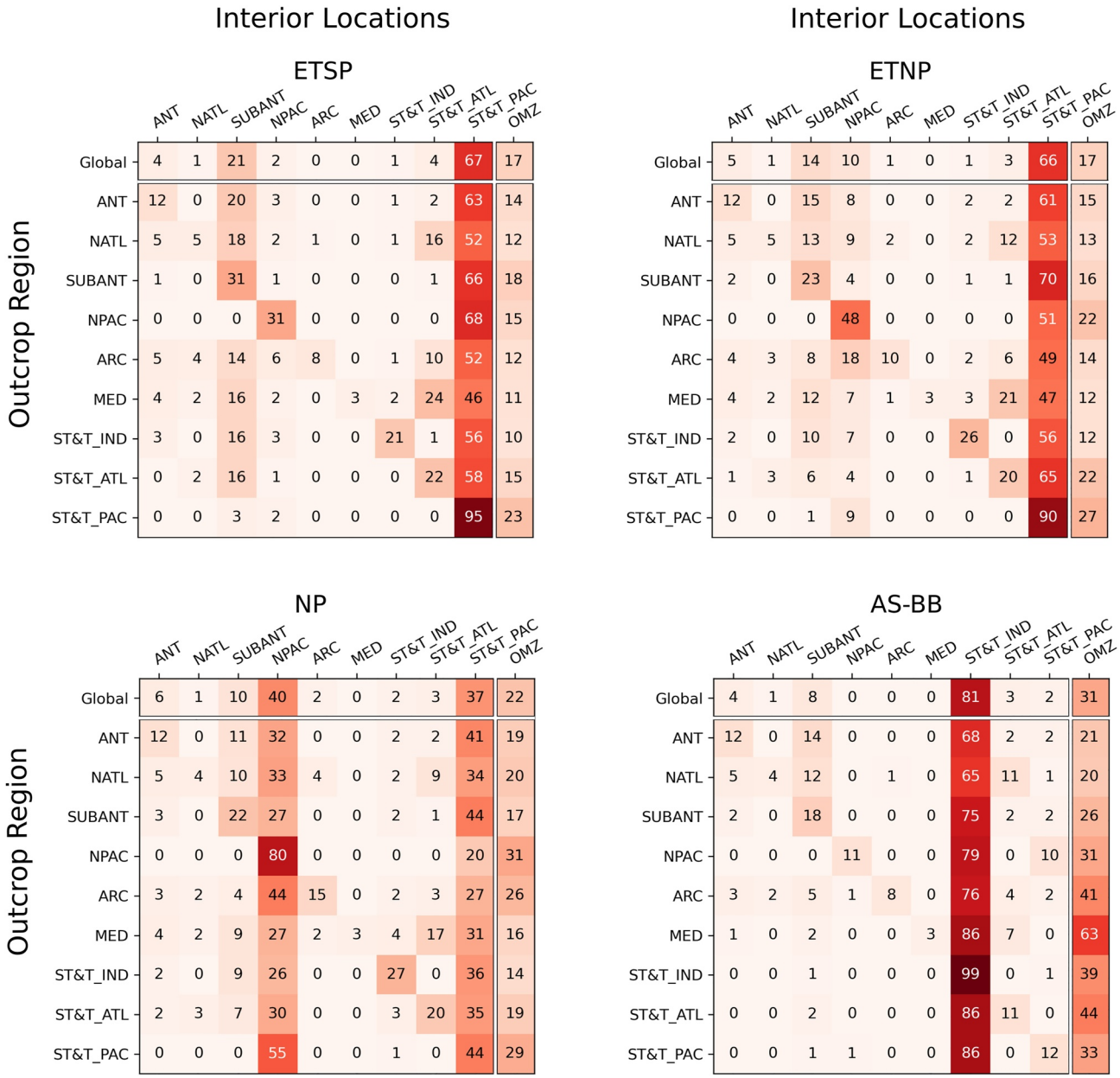

Figure 8. Regional oxygen consumption along the pathways from outcrop regions to each of the Oxygen Minimum Zones (OMZs), $\overrightarrow{\Delta O_2}$, as a percentage of the total pathway integrated deficit. Every row sums to 100% (excluding rounding errors) and includes consumption within the OMZs. The percentage of the remineralization that occurs within the OMZs is added as an extra column. The selected outcrop regions are the Antarctic (ANT), North Atlantic (NATL), Subantarctic (SUBANT), North Pacific (NPAC), Arctic (ARC), Mediterranean Sea (MED), Subtropical and Tropical Indian (ST&T_IND), Subtropical and Tropical Atlantic (ST&T_ATL) and Subtropical and Tropical Pacific (ST&T_PAC).

the Subantarctic region. The depth of the pathway relative to the remineralization profile determines the oxygen consumption in each region.

It is well known that most of the remineralization occurs in the upper 1,000 m of the water column, as organic particles sink. The most labile particles are rapidly remineralized in the upper ocean, while only the most refractory particles reach the bottom (DeVries & Weber, 2017; Martin et al., 1987). This is reflected in the attenuation of particulate carbon fluxes, that follow a power law distribution known as the Martin curve (Martin et al., 1987). When the global ocean is taken as destination Ω, the TMI conforms to the general remineralization profile, having its largest oxygen sinks around 500 m. About 39% of the global oxygen utilization, $\overrightarrow{\Delta O_2}$, occurs in the upper

1,000 m, close to the 44% occurring at 1,000–3,000 m, with a substantial 17% taking place below 3,000 m (Figure S4 in Supporting Information S1), which is in excellent agreement with the 18% estimated by Holzer (2022). However, the shape of the curve is not identical in every region as a result of the relationship between the remineralization rate and temperature and oxygen (DeVries & Weber, 2017). As such, in colder regions, the remineralization rate is slower because of a lower metabolic index, and as a result, the curve is more gentle than in warmer regions (Marsay et al., 2015). Similarly, in regions where oxygen is not available, such as the OMZs, the metabolic index also decreases and the remineralization curve is more gentle (Devol & Hartnett, 2001). Cold and oxygen-depleted regions thus translate into high transfer efficiency, that is, the fraction of particulate carbon export that survives remineralization above 1,000 m (DeVries & Weber, 2017). The general remineralization profiles for the oxygen-deficit in the OMZs (the along-path oxygen utilization $\overrightarrow{\Delta O_2}$ when OMZs are Ω), also show the characteristic power law distribution from the Martin curve. Individual pathways, however, vary substantially. High latitude cold endmembers, such as the Antarctic and North Atlantic show a more depth-independent $\overrightarrow{\Delta O_2}$ profile. Conversely, in the tropical and subtropical pathways, remineralization occurs mostly in the upper ocean. Thus, the presence of colder waters allows a larger, deeper export of carbon and remineralization.

Because most of the $\overrightarrow{\Delta O_2}$ occurs in the upper 1,000 m, if the pathway for an endmember lies below the remineralization curve (Figure 9) the oxygen would be relatively preserved until resurfacing. This is the case for distant endmembers—for example, the North Atlantic, where the largest concentration of $\overrightarrow{\Delta O_2}$ are at the OMZs (Figures S5–S8 in Supporting Information S1). This preservation of oxygen reinforces the idea that, in steady-state, OMZs are primarily set by the geometry of the oceanic pathways that upwell old water with relatively low-oxygen concentrations to the OMZs, where the final remineralization and push toward suboxic (<20 μmol kg^{-1}) conditions occur.

4. Discussion

Our results agree well with other studies that use similar approaches to either determine the ventilation times-scales of OMZs or determine the fate of the oxygen in the ocean. Fu, Bardin, and Primeau (2018) used a transport matrix based on a General Circulation Model to determine the mixed layer ventilation regions of OMZs. While the general pattern of our results in terms of both volume and timescales agree with theirs, there are differences regarding the importance and formation regions of Antarctic Bottom Water. We estimate that more than 20% of the water in the ETSP and ETNP correspond to Antarctic endmembers while Fu, Bardin, and Primeau (2018) estimated that only 3.8% and 8.1%, respectively, was formed south of 55°S. The spatial pattern also differs. While the Antarctic Bottom Water formation in the TMI occurs in the Ross and Weddell Sea, in Fu, Bardin, and Primeau (2018) it occurs exclusively along the shelf. This difference might be due to an incomplete model spin-up (Fu, Bardin, & Primeau, 2018) but more generally it is likely also related to how the Antarctic Bottom Water is represented in models, as Earth System Models struggle to correctly represent the formation of Antarctic Bottom Water, and also North Atlantic Deep Water (Heuzé, 2017, 2021). In particular, although the Community Earth System Model (CESM) model used to construct the transport matrix in Fu, Bardin, and Primeau (2018) correctly represents bottom water properties, its Pacific Meridional Overturning Circulation is too shallow (Supplementary Material in Cabré et al., 2015) compared to observations (Holzer et al., 2021). The TMI uses observations directly to constrain the advective-diffusive transport, and the ventilation pathways, and water mass fractions of both the Antarctic Bottom Water and the North Atlantic Deep Water are comparable to other observation-based estimates (DeVries & Primeau, 2011; Gebbie & Huybers, 2010; Holzer et al., 2021). In the NP OMZ, our estimates of the fractions of Antarctic Bottom Water and North Atlantic Deep Water agree well with the recent estimates by Holzer et al. (2021), who argue that regions such as the Shadow Zone in the NP to a large extent is ventilated by Antarctic Bottom Water and North Atlantic Deep Water and controlled by diffusion. Most importantly, Fu, Bardin, and Primeau (2018) quantified only the transport of volume, while here we also determine the transport of oxygen and oxygen-deficit.

The fate of the oxygen in the ocean was recently explored by Holzer (2022) who determined the origins of the oxygen-deficit in the interior ocean based on the OCIM2 transport matrix (DeVries & Holzer, 2019). While some of their results are directly comparable to ours, there are a few key differences that are worth pointing out. The TMI estimates the total oxygen-deficit in each interior location $\left(\overrightarrow{\Delta O_2}\right)$ directly from the tracer distributions, whereas Holzer (2022) estimated $\overrightarrow{\Delta O_2}$ by tracing TOU back in time by reversing the advective-diffusive

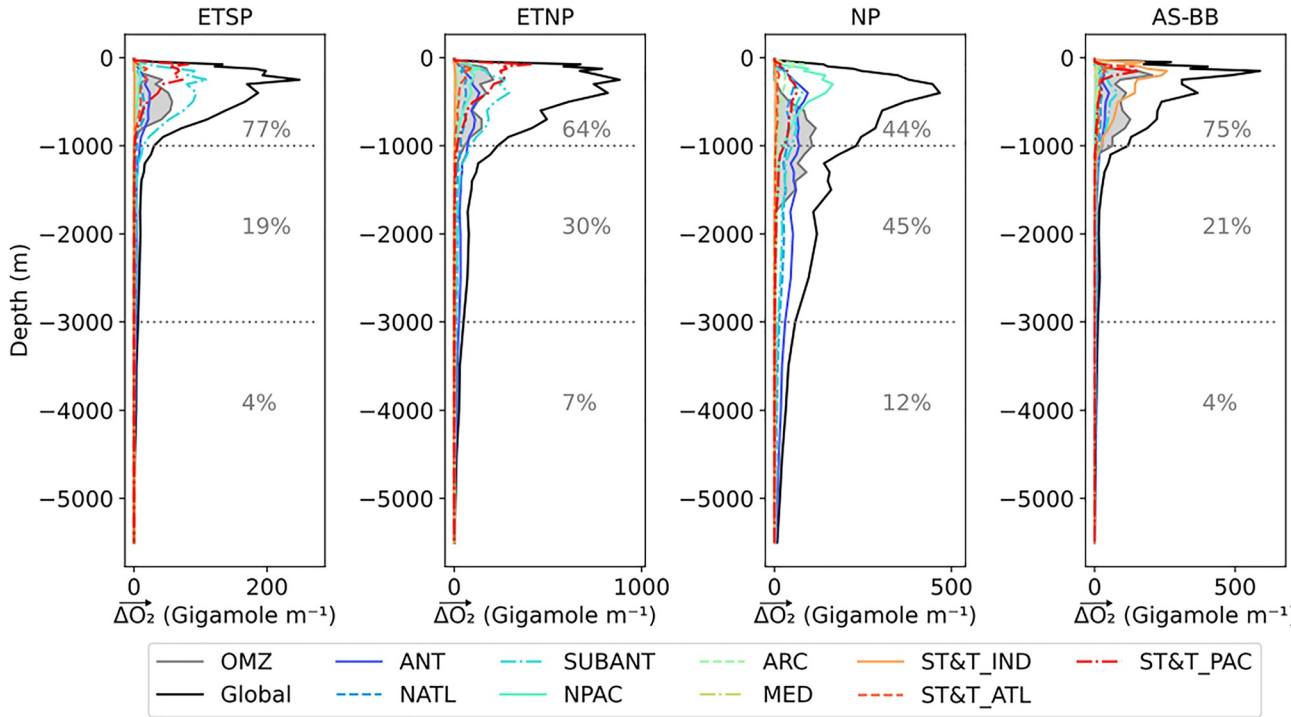

Figure 9. Along-path oxygen utilization $\left(\overrightarrow{\Delta O_2}\right)$ per meter depth for each specific pathway for each endmember, globally integrated. The colors indicate the different endmembers and gray shading represents the $\overrightarrow{\Delta O_2}$ that occurs within the Oxygen Minimum Zone, while the numbers indicate the percentage of the total $\overrightarrow{\Delta O_2}$ originating at each of the depth intervals. The endmembers selected are the Antarctic (ANT), North Atlantic (NATL), Subantarctic (SUBANT), North Pacific (NPAC), Arctic (ARC), Mediterranean Sea (MED), Subtropical and Tropical Indian (ST&T_IND), Subtropical and Tropical Atlantic (ST&T_ATL) and Subtropical and Tropical Pacific (ST&T_PAC).

transport. Thus, both studies converge on the same solution but start at opposite ends. In addition, the biogeochemical model used by Holzer (2022) is parameterized with a Martin power law with a globally uniform exponent and therefore there are no spatial variations in particle transfer efficiency. Our remineralization pathways and the along-path oxygen utilization presented in Section 3.2 are equivalent to Figure 5 in Holzer (2022). Both show a very similar pattern and magnitude. The strongest oxygen loss occurs in OMZs because the fraction of volume that would reach the OMZs is also higher. Contrarily, afar from the OMZs, the fraction of volume at each grid cell that reaches the OMZs is much lower (Figure S3 in Supporting Information S1) which results in a smaller $\overrightarrow{\Delta O_2}$ per grid cell. However, when this is integrated, the total amount of oxygen-deficit is larger than the one originating in the OMZs. Our results also show that, surprisingly, the North Atlantic and Arctic contribute substantially to the oxygen in the NP OMZ (Figure 4). This is also supported by Holzer (2022) who found substantial fluxes of atmospheric oxygen into the North Atlantic that is bound to be utilized within the NP Hypoxic Zone.

While it is clear that OMZs are expanding (Stramma et al., 2010; Zhou et al., 2022), the driving mechanisms are still an area of active research. The warming of the surface ocean impacts the oxygen concentrations directly by decreasing the solubility of oxygen, and indirectly by increasing ocean stratification. Approximately 15% of the observed oxygen loss is explained by the warming of the mixed layer (Helm et al., 2011). The response of OMZs to warming must unfold on decadal to centennial timescales according their ventilation timescales identified here. This might be a reason why the changes in dissolved oxygen and temperature for the last decade are not correlated (Stramma & Schmidtko, 2021), indicating that changes in biology and/or circulation dominate (Ito et al., 2016). As we show here, in steady-state, OMZs are most sensitive to changes in remineralization in the Subtropical and Tropical waters (Figure 7), but nevertheless, remote large-scale changes (especially in the Southern Ocean) would still impact greatly, albeit on longer timescales (Keller et al., 2016). This also has important implications as Subtropical gyres and the Southern Ocean are regions where iron fertilization is considered as a Carbon Dioxide Removal strategy (Oschlies et al., 2010; Yoon et al., 2018). The increased remineralization resulting from fertilization would eventually increase the oxygen deficiency in the already oxygen-depleted OMZs.

Table 1
Percent Volume, Oxygen and Oxygen-Deficit Contributions to Each Oxygen Minimum Zone From Each Source Region: Antarctic Marginal Seas (ANT), North Atlantic (NATL), Subantarctic (SUBANT), North Pacific (NPAC), Arctic (ARC), Mediterranean (MED), Subtropics and Tropics (ST&T)

	ETSP	ETNP	NP	AS-BB
Volume (%)				
ANT	17	24	31	17
NATL	8	11	16	9
SUBANT	46	30	15	16
NPAC	2	8	17	1
ARC	2	3	6	5
MED	0	1	1	4
ST&T	24	24	14	47
Oxygen (%)				
ANT	3	4	1	1
NATL	0	3	14	1
SUBANT	67	23	0	13
NPAC	1	30	50	2
ARC	0	3	17	29
MED	0	0	0	7
ST&T	28	38	18	57
Oxygen utilized (%)				
ANT	20	27	35	20
NATL	10	13	18	12
SUBANT	45	30	16	18
NPAC	3	7	14	1
ARC	2	3	6	5
MED	0	0	1	4
ST&T	18	18	11	41

Note. ST&T is the sum of contributions from the Atlantic, Pacific and Indian Subtropical and Tropical basins.

While we believe the TMI gives an appropriate representation of the origins of OMZs, despite the differences in the modeled and observed OMZs, a number of improvements should be made to better fit the observations. Flexible stoichiometric ratios would allow the TMI to constrain the impacts of remineralization in suboxic environments more accurately. Additionally, pointwise observations could be used instead of relying on already gridded products that might transfer their own biases to the TMI. With enough observations, a higher resolution TMI could be constrained, which would also improve the pathways (Brakstad et al., 2023). In addition, the TMI is a steady-state approach and the findings presented here should be taken as such, that is, no variability or feedbacks are accounted for. Constraining a seasonally varying TMI could allow primary production and water mass formation to co-vary, thus providing further insights on impacts of circulation and primary production on OMZs. Similarly, constraining circulation at decadal frequencies might enable investigations of these processes in the context of a changing climate. The global decadal repeat hydrography program GO-SHIP, as well as the Biogeochemical Argo program, may provide the necessary observations for such a purpose. A special focus should be placed on deep measurements, as such observations are needed to shed further light on the old and cold remote origins of OMZs.

5. Conclusions

In this study, we show that the world's OMZs are ventilated by mode, intermediate and deep waters formed at high latitudes. Of particular importance are the Subantarctic region (by means of the Mode/Intermediate Waters) and the Antarctic region (via Antarctic Bottom Water; Table 1). These waters supply up to half of the volume for every OMZ in the Pacific (and to a lesser extent to the AS-BB OMZ). However, OMZs are mostly oxygenated by Subtropical and Tropical, Subantarctic Mode/Intermediate and NP Intermediate waters, on decadal to centennial timescales, respectively. High-latitude endmembers, Antarctic regions and the North Atlantic ventilate OMZs on longer (millennial) timescales and most of the oxygen is utilized upon arrival to the subtropical and tropical regions. These waters thus contribute to most of the volume and have relatively low oxygen concentrations. Therefore they contribute strongly to the oxygen-deficit of OMZs. Our results are in agreement with earlier studies that suggested that OMZs are set by the transport of low-oxygen waters into OMZs (Czeschel et al., 2011; Olson et al., 1993; Sonnerup et al., 2019).

Here, we propose a mechanism that summarizes the formation of the oxygen-deficit in the OMZs in steady-state (i.e., without changes in solubility or biology). Only a small quantity of oxygen is utilized in the formation regions at high latitudes, where waters are subducted. Due to the long pathways that pass through the deep ocean, the relatively low oxygen utilization adds up to about half of the oxygen-deficit before these waters reach the Subtropical and Tropical regions. Here is where most of the oxygen-deficit originates, with the strongest oxygen utilization occurring within the OMZs upon upwelling. This is also the case for remote endmembers (e.g., North Atlantic) that preserve substantial amounts of oxygen that are only utilized when reaching the OMZs. Thus, our study highlights the delicate balance in oxygen loss that results in the OMZs, where the oxygen-deficit originating away from the OMZs is of similar magnitude to that originating around (subtropics and tropics) and within the OMZs. Our results suggest that the OMZs are set by the geometry of the ocean circulation pathways that upwell old and relatively low-oxygen waters, however, the presented pattern may change as a result of changes in solubility and biology due to the changing climate.

Acronyms

OMZ	Oxygen Minimum Zone
ETSP	East Tropical South Pacific

ETNP	East Tropical North Pacific
NP	North Pacific
AS-BB	Arabian Sea—Bay of Bengal

Data Availability Statement

The TMI transport matrix as well as the tracers distributions that are used to generate the results in this paper are available in Gebbie et al. (2023) (DOI: 10.5281/zenodo.8226802).

Acknowledgments

We thank three anonymous reviewers for their careful and constructive reviews. XD was supported by a PhD research fellowship from the University of Bergen. AO and SKL appreciate the support from the Research Council of Norway (ICOS-Norway, project number 245972) and OceanICU, Improving Carbon Understanding funded by the Horizon Europe research and innovation program under grant agreement No 101083922. ELM was supported by UKRI grants Atlantic Biogeochemical (ABC) fluxes (ref no. NE/M005046/2) and TICTOC:Transient tracer-based Investigation of Circulation and Thermal Ocean Change (ref no. NE/P019293/2). AB was supported by the Trond Mohn Foundation under grant agreement BFS2016REK01. GG was supported by U.S. NSF Grant OCE-1850753 and OCE-2122805.

References

Anderson, L. A., & Sarmiento, J. L. (1994). Redfield ratios of remineralization determined by nutrient data analysis. *Global Biogeochemical Cycles*, *8*(1), 65–80. https://doi.org/10.1029/93GB03318

Bianchi, D., Dunne, J. P., Sarmiento, J. L., & Galbraith, E. D. (2012). Data-based estimates of suboxia, denitrification, and N_2O production in the ocean and their sensitivities to dissolved O_2. *Global Biogeochemical Cycles*, *26*(March), 1–13. https://doi.org/10.1029/2011GB004209

Brakstad, A., Gebbie, G., Våge, K., Jeansson, E., & Ólafsdóttir, S. R. (2023). Formation and pathways of dense water in the Nordic Seas based on a regional inversion. *Progress in Oceanography*, *212*, 102981. https://doi.org/10.1016/j.pocean.2023.102981

Busecke, J. J. M., Resplandy, L., Ditkovsky, S. J., & John, J. G. (2022). Diverging fates of the Pacific Ocean oxygen minimum zone and its core in a warming world. *AGU Advances*, *3*(6), e2021AV000470. https://doi.org/10.1029/2021AV000470

Cabré, A., Marinov, I., Bernardello, R., & Bianchi, D. (2015). Oxygen minimum zones in the tropical Pacific across CMIP5 models: Mean state differences and climate change trends. *Biogeosciences*, *12*(18), 5429–5454. https://doi.org/10.5194/bg-12-5429-2015

Carter, B. R., Feely, R. A., Lauvset, S. K., Olsen, A., DeVries, T., & Sonnerup, R. (2021). Preformed properties for marine organic matter and carbonate mineral cycling quantification. *Global Biogeochemical Cycles*, *35*(1), e2020GB006623. https://doi.org/10.1029/2020GB006623

Czeschel, R., Stramma, L., Schwarzkopf, F. U., Giese, B. S., Funk, A., & Karstensen, J. (2011). Middepth circulation of the eastern tropical South Pacific and its link to the oxygen minimum zone. *Journal of Geophysical Research*, *116*(1), 1–13. https://doi.org/10.1029/2010JC006565

De Lavergne, C., Madec, G., Roquet, F., Holmes, R. M., & McDougall, T. J. (2017). Abyssal Ocean overturning shaped by seafloor distribution. *Nature*, *551*(7679), 181–186. https://doi.org/10.1038/nature24472

Deutsch, C., Brix, H., Ito, T., Frenzel, H., & Thompson, L. (2011). Climate-forced variability of ocean hypoxia. *Science*, *333*(6040), 336–339. https://doi.org/10.1126/science.1202422

Devol, A. H., & Hartnett, H. E. (2001). Role of the oxygen-deficient zone in transfer of organic carbon to the deep ocean. *Limnology and Oceanography*, *46*(7), 1684–1690. https://doi.org/10.4319/lo.2001.46.7.1684

DeVries, T., Deutsch, C., Primeau, F., Chang, B., & Devol, A. (2012). Global rates of water-column denitrification derived from nitrogen gas measurements. *Nature Geoscience*, *4*(August), 547–550. https://doi.org/10.1038/ngeo1515

DeVries, T., & Holzer, M. (2019). Radiocarbon and helium isotope constraints on deep ocean ventilation and mantle-3He sources. *Journal of Geophysical Research: Oceans*, *124*(5), 3036–3057. https://doi.org/10.1029/2018JC014716

DeVries, T., & Primeau, F. (2011). Dynamically and observationally constrained estimates of water-mass distributions and ages in the global ocean. *Journal of Physical Oceanography*, *41*(12), 2381–2401. https://doi.org/10.1175/JPO-D-10-05011.1

DeVries, T., & Weber, T. (2017). The export and fate of organic matter in the ocean: New constraints from combining satellite and oceanographic tracer observations. *Global Biogeochemical Cycles*, *31*(3), 535–555. https://doi.org/10.1002/2016GB005551

Frölicher, T. L., Aschwanden, M. T., Gruber, N., Jaccard, S. L., Dunne, J. P., & Paynter, D. (2020). Contrasting upper and deep ocean oxygen response to protracted global warming. *Global Biogeochemical Cycles*, *34*(8), e2020GB006601. https://doi.org/10.1029/2020GB006601

Fu, W., Bardin, A., & Primeau, F. (2018). Tracing ventilation source of tropical pacific oxygen minimum zones with an adjoint global ocean transport model. *Deep-Sea Research Part I: Oceanographic Research Papers*, *139*(November 2017), 95–103. https://doi.org/10.1016/j.dsr.2018.07.017

Fu, W., Primeau, F., Keith Moore, J., Lindsay, K., & Randerson, J. T. (2018). Reversal of increasing tropical ocean hypoxia trends with sustained climate warming. *Global Biogeochemical Cycles*, *32*(4), 551–564. https://doi.org/10.1002/2017GB005788

Fuenzalida, R., Schneider, W., Garcés-Vargas, J., Bravo, L., & Lange, C. (2009). Vertical and horizontal extension of the oxygen minimum zone in the eastern South Pacific Ocean. *Deep-Sea Research Part II: Topical Studies in Oceanography*, *56*(16), 992–1003. https://doi.org/10.1016/j.dsr2.2008.11.001

Gebbie, G., Hamilton, B. R., & Davila, X. (2023). TMI.jl: Total Matrix Intercomparison software tools for global ocean circulation (v0.2.0). *Zenodo*. https://doi.org/10.5281/zenodo.8226802

Gebbie, G., & Huybers, P. (2010). Total matrix intercomparison: A method for determining the geometry of water-mass pathways. *Journal of Physical Oceanography*, *40*(8), 1710–1728. https://doi.org/10.1175/2010jpo4272.1

Gebbie, G., & Huybers, P. (2011). How is the ocean filled?. *Geophysical Research Letters*, *38*(February), 1–5. https://doi.org/10.1029/2011GL046769

Gebbie, G., & Huybers, P. (2012). The mean age of ocean waters inferred from radiocarbon observations: Sensitivity to surface sources and accounting for mixing histories. *Journal of Physical Oceanography*, *42*(2), 291–305. https://doi.org/10.1175/jpo-d-11-043.1

Gouretski, V., & Koltermann, K. P. (2004). *WOCE global hydrographic climatology* (Berichte des Bundesamtes für Seeschifffahrt und Hydrographie Tech. Rep. 35). Digital Media.

Gray, J. S., Wu, R. S. S., & Ying, Y. O. (2002). Effects of hypoxia and organic enrichment on the coastal marine environment. *Marine Ecology Progress Series*, *238*, 249–279. https://doi.org/10.3354/meps238249

Haine, T. W., & Hall, T. M. (2002). A generalized transport theory: Water-mass composition and age. *Journal of Physical Oceanography*, *32*(6), 1932–1946. https://doi.org/10.1175/1520-0485(2002)032<1932:AGTTWM>2.0.CO;2

Helly, J. J., & Levin, L. A. (2004). Global distribution of naturally occurring marine hypoxia on continental margins. *Deep-Sea Research Part I: Oceanographic Research Papers*, *51*(9), 1159–1168. https://doi.org/10.1016/j.dsr.2004.03.009

Helm, K. P., Bindoff, N. L., & Church, J. A. (2011). Observed decreases in oxygen content of the global ocean. *Geophysical Research Letters*, *38*(23), 1–6. https://doi.org/10.1029/2011GL049513

Heuzé, C. (2017). North Atlantic deep water formation and AMOC in CMIP5 models. *Ocean Science Discussions*, *13*(4), 1–22. https://doi.org/10.5194/os-2017-2

Heuzé, C. (2021). Antarctic bottom water and north Atlantic deep water in CMIP6 models. *Ocean Science*, *17*(1), 59–90. https://doi.org/10.5194/os-17-59-2021

Holzer, M. (2022). The fate of oxygen in the ocean and its sensitivity to local changes in biological production. *Journal of Geophysical Research: Oceans*, *127*(8), e2022JC018802. https://doi.org/10.1029/2022jc018802

Holzer, M., DeVries, T., & de Lavergne, C. (2021). Diffusion controls the ventilation of a Pacific Shadow Zone above abyssal overturning. *Nature Communications*, *12*(1), 4348. (Number: 1). https://doi.org/10.1038/s41467-021-24648-x

Ito, T., Follows, M. J., & Boyle, E. A. (2004). Is AOU a good measure of respiration in the oceans? *Geophysical Research Letters*, *31*(17), 1–4. https://doi.org/10.1029/2004GL020900

Ito, T., Nenes, A., Johnson, M. S., Meskhidze, N., & Deutsch, C. (2016). Acceleration of oxygen decline in the tropical Pacific over the past decades by aerosol pollutants. *Nature Geoscience*, *9*(6), 443–447. https://doi.org/10.1038/ngeo2717

Johnson, G. C. (2008). Quantifying Antarctic bottom water and North Atlantic deep water volumes. *Journal of Geophysical Research*, *113*(C5), C05027. https://doi.org/10.1029/2007JC004477

Jones, D. C., Meijers, A. J. S., Shuckburgh, E., Sallée, J.-B., Haynes, P., McAufield, E. K., & Mazloff, M. R. (2016). How does subantarctic mode water ventilate the southern hemisphere subtropics? *Journal of Geophysical Research: Oceans*, *121*(9), 6558–6582. https://doi.org/10.1002/2016JC011680

Kalvelage, T., Lavik, G., Lam, P., Contreras, S., Arteaga, L., Löscher, C. R., et al. (2013). Nitrogen cycling driven by organic matter export in the South Pacific oxygen minimum zone. *Nature Geoscience*, *6*(February), 228–234. https://doi.org/10.1038/ngeo1739

Karstensen, J., Stramma, L., & Visbeck, M. (2008). Oxygen minimum zones in the eastern tropical Atlantic and Pacific oceans. *Progress in Oceanography*, *77*(4), 331–350. https://doi.org/10.1016/j.pocean.2007.05.009

Keeling, R. F., & Garcia, H. E. (2002). The change in oceanic O_2 inventory associated with recent global warming. *Proceedings of the National Academy of Sciences*, *99*(12), 7848–7853. https://doi.org/10.1073/pnas.122154899

Keeling, R. F., Körtzinger, A., & Gruber, N. (2010). Ocean deoxygenation in a warming world. *Annual Review of Marine Science*, *2*(1), 199–229. https://doi.org/10.1146/annurev.marine.010908.163855

Keller, D. P., Kriest, I., Koeve, W., & Oschlies, A. (2016). Southern Ocean biological impacts on global ocean oxygen. *Geophysical Research Letters*, *43*(12), 6469–6477. https://doi.org/10.1002/2016GL069630

Key, R. M., Kozyr, A., Sabine, C. L., Lee, K., Wanninkhof, R., Bullister, J. L., et al. (2004). A global ocean carbon climatology: Results from Global Data Analysis Project (GLODAP). *Global Biogeochemical Cycles*, *18*(4), 1–23. https://doi.org/10.1029/2004GB002247

Luyten, J. R., Pedlosky, J., & Stommel, H. (1983). The ventilated thermocline. *Journal of Physical Oceanography*, *13*(2), 292–309. https://doi.org/10.1175/1520-0485(1983)013<0292:TVT>2.0.CO;2

Marsay, C. M., Sanders, R. J., Henson, S. A., Pabortsava, K., Achterberg, E. P., & Lampitt, R. S. (2015). Attenuation of sinking particulate organic carbon flux through the mesopelagic ocean. *Proceedings of the National Academy of Sciences*, *112*(4), 1089–1094. https://doi.org/10.1073/pnas.1415311112

Martin, J. H., Knauer, G. A., Karl, D. M., & Broenkow, W. W. (1987). VERTEX: Carbon cycling in the north east Pacific. *Deep-Sea Research*, *34*(2), 267–285. https://doi.org/10.1016/0198-0149(87)90086-0

Olson, D. B., Hitchcock, G. L., Fine, R. A., & Warren, B. A. (1993). Maintenance of the low-oxygen layer in the central Arabian Sea. *Deep-Sea Research Part II*, *40*(3), 673–685. https://doi.org/10.1016/0967-0645(93)90051-N

Oschlies, A., Koeve, W., Rickels, W., & Rehdanz, K. (2010). Side effects and accounting aspects of hypothetical large-scale Southern Ocean iron fertilization. *Biogeosciences*, *7*(12), 4017–4035. https://doi.org/10.5194/bg-7-4017-2010

Paulmier, A., & Ruiz-Pino, D. (2009). Oxygen minimum zones (OMZs) in the modern ocean. *Progress in Oceanography*, *80*(3–4), 113–128. https://doi.org/10.1016/j.pocean.2008.08.001

Primeau, F., & Holzer, M. (2006). The ocean's memory of the atmosphere: Residence-time and ventilation-rate distributions of water masses. *Journal of Physical Oceanography*, *36*(7), 1439–1456. https://doi.org/10.1175/JPO2919.1

Shimizu, Y., Iwao, T., Yasuda, I., Ito, S. I., Watanabe, T., Uehara, K., et al. (2004). Formation process of North Pacific intermediate water revealed by profiling floats set to drift on 26.7σQ isopycnal surface. *Journal of Oceanography*, *60*(2), 453–462. https://doi.org/10.1023/B:JOCE.0000038061.55914.eb

Sloyan, B. M., Talley, L. D., Chereskin, T. K., Fine, R., & Holte, J. (2010). Antarctic intermediate water and subantarctic mode water formation in the Southeast Pacific: The role of turbulent mixing. *Journal of Physical Oceanography*, *40*(7), 1558–1574. https://doi.org/10.1175/2010JPO4114.1

Smethie, W. M. (1987). Nutrient regeneration and denitrification in low oxygen fjords. *Deep-Sea Research Part I: Oceanographic Research Papers*, *34*(5–6), 983–1006. https://doi.org/10.1016/0198-0149(87)90049-5

Sonnerup, R. E., Chang, B. X., Warner, M. J., & Mordy, C. W. (2019). Timescales of ventilation and consumption of oxygen and fixed nitrogen in the eastern tropical South Pacific oxygen deficient zone from transient tracers. *Deep-Sea Research Part I: Oceanographic Research Papers*, *151*(July), 103080. https://doi.org/10.1016/j.dsr.2019.103080

Stramma, L., Johnson, G. C., Firing, E., & Schmidtko, S. (2010). Eastern Pacific oxygen minimum zones: Supply paths and multidecadal changes. *Journal of Geophysical Research*, *115*(9), 1–12. https://doi.org/10.1029/2009JC005976

Stramma, L., & Schmidtko, S. (2021). Tropical deoxygenation sites revisited to investigate oxygen and nutrient trends. *Ocean Science*, *17*(3), 833–847. https://doi.org/10.5194/os-17-833-2021

Teng, Y.-C., Primeau, F. W., Moore, J. K., Lomas, M. W., & Martiny, A. C. (2014). Global-scale variations of the ratios of carbon to phosphorus in exported marine organic matter. *Nature Geoscience*, *7*(12), 895–898. https://doi.org/10.1038/ngeo2303

Yoon, J.-E., Yoo, K.-C., Macdonald, A. M., Yoon, H.-I., Park, K.-T., Yang, E. J., et al. (2018). Reviews and syntheses: Ocean iron fertilization experiments – Past, present, and future looking to a future Korean Iron Fertilization Experiment in the Southern Ocean (KIFES) project. *Biogeosciences*, *15*(19), 5847–5889. https://doi.org/10.5194/bg-15-5847-2018

Zhou, Y., Gong, H., & Zhou, F. (2022). Responses of horizontally expanding oceanic oxygen minimum zones to climate change based on observations. *Geophysical Research Letters*, *49*(6), 1–11. https://doi.org/10.1029/2022GL097724